NASA
Technical
Paper
1798

November 1981

Effect of Fuel-Air-Ratio Nonuniformity on Emissions of Nitrogen Oxides

Valerie J. Lyons

NASA

NASA
Technical
Paper
1798

1981

Effect of Fuel-Air-Ratio Nonuniformity on Emissions of Nitrogen Oxides

Valerie J. Lyons
Lewis Research Center
Cleveland, Ohio

National Aeronautics
and Space Administration

**Scientific and Technical
Information Branch**

Summary

An analytical and experimental study was performed to determine how inlet fuel-air-ratio nonuniformity affects emissions of nitrogen oxides (NO_x). The theoretical NO_x levels were verified in a flametube rig at inlet air temperatures of 600, 700, and 800 K, a rig pressure of 0.3 MPa, a reference velocity of 25 meters per second, an overall equivalence ratio of 0.6, and a residence time near 0.002 second.

The theory predicts an increase in NO_x emissions with increased fuel-air-ratio nonuniformity for average equivalence ratios less than 0.7 and a decrease in NO_x emissions for average equivalence ratios near stoichiometric.

The results of this report can be used to predict the degree of uniformity of fuel-air-ratio profiles that is necessary to achieve NO_x emissions goals for actual engines that use lean, premixed, prevaporized combustion systems.

Introduction

This report presents the results of an analytical and experimental study to determine how the degree of nonuniformity in the incoming fuel-air-ratio profile affects emissions of nitrogen oxides (NO_x).

Because of rising fuel and maintenance costs and regulations governing exhaust emissions from gas turbine engines (ref. 1), interest has arisen in advancing combustor technology. Several studies (refs. 2 to 5) have explored ways of advancing combustor technology to meet these demands. A promising concept for reducing engine emissions and obtaining superior performance and high durability is lean, premixed, prevaporized (LPP) combustion. A number of flametube studies (refs. 6 to 11) have demonstrated that in an LPP environment an order-of-magnitude reduction in NO_x levels can be attained while achieving 99 percent combustion efficiency.

This LPP combustion concept formed the basis of the NASA Advanced Low Emission Combustor program (ref. 12). The purpose of this program is to evolve the technology of lean, premixed, prevaporized combustion into a practical aircraft gas turbine combustion system that exhibits superior performance, high durability, fuel flexibility, and environmentally acceptable pollutant emissions over the entire flight envelope. Although the LPP concept shows great promise for reducing NO_x emissions, several practical problems are associated with its application. These problems include blowout, altitude relight, autoignition, flashback, and achieving satisfactory premixing and prevaporization.

In a practical application of LPP combustion it may not be feasible to fully premix the fuel and air before burning occurs. A fully premixed system would be equivalent to a uniform fuel-air-ratio profile. Any lack of mixing would produce nonuniform fuel-air-ratio profiles. An analytical study of the effect of nonuniformity on NO_x emissions has been undertaken (ref. 13). A slightly different presentation of the theory of NO_x production in a nonuniform fuel-air mixture is presented herein. Experimental data were taken to verify the theory.

To define what degree of premixing may be required in an LPP system in order to produce acceptably low NO_x emissions, several nonuniform, but fully vaporized, fuel-air-ratio inlet profiles were studied. The incoming fuel-air-ratio profiles were made nonuniform across the flametube rig by varying the amount of fuel to different zones of a multipoint fuel injector. The spatial fuel distribution and exhaust emissions were determined from measurements taken by a radially traversing probe downstream of a water-cooled, perforated-plate flameholder. For each of the inlet air temperatures of 600, 700, and 800 K, six fuel-air-ratio profiles were studied. Data were obtained in a flametube rig at a reference velocity of 25 meters per second and a rig pressure of 0.3 megapascal. Jet A fuel was used.

Theory and Analysis

In applying lean, premixed, prevaporized combustion to actual gas turbine engines, it may not be possible to uniformly premix the fuel and inlet air. Using any fuel injection system with discrete injection points will produce relatively fuel-rich and fuel-lean zones that may still be present when combustion occurs.

Theoretical Calculations

In a flametube rig the fuel-air distribution can be shown by a plot of local equivalence ratio (the ratio

of the local fuel-air ratio to the stoichiometric) φ_l as a function of the pipe radius r. If axial symmetry and uniform air density are assumed and a constant air-velocity profile exists, the average equivalence ratio for a φ_l–r profile is

$$\bar{\varphi} = \frac{\int_0^{r_{max}} \varphi_l r \, dr}{\int_0^{r_{max}} r \, dr} \tag{1}$$

where r_{max} is half the pipe inner diameter.

The degree of nonuniformity of the profile can be described by a nonuniformity parameter

$$s = \left[\frac{\int_0^{r_{max}} (\varphi_l - \bar{\varphi})^2 r \, dr}{\int_0^{r_{max}} r \, dr} \right]^{1/2} \tag{2}$$

Basically, this nonuniformity parameter s is the standard deviation from the mean of the local equivalence ratio distribution. (Note that this s parameter is different from the s parameter used by Mikus, Heywood, and Hicks; in their similar study in reference 13, their s was the standard deviation divided by the mean equivalence ratio.)

Two methods of determining an average theoretical value of NO_x were used. The first method required obtaining an experimental φ_l distribution and then predicting a NO_x level for each measured φ_l from the well-stirred-reactor program described in reference 14. The second method does not need experimental data. Instead it is assumed that a Gaussian distribution of φ_l exists that has the same $\bar{\varphi}$ and s as the corresponding experimental results.

Once proven reliable the Gaussian method can be used to predict NO_x levels without experimental data. All that would be needed to predict the average NO_x level would be an estimate of the average equivalence ratio $\bar{\varphi}$ and degree of nonuniformity s for the combustion system. In the Gaussian method the well-stirred-reactor program of reference 14 was used to predict local NO_x values for a set of equivalence ratios at the given inlet air temperature and pressure and combustor residence time. These NO_x values were then weighted by a Gaussian distribution function

$$f(\varphi_l) = \frac{1}{\sqrt{2\pi}\, s} \exp\left[\frac{-(\varphi_l - \bar{\varphi})^2}{2s^2} \right] \tag{3}$$

The predicted value of NO_x for the given nonuniform profile described by s and the Gaussian distribution is

$$(NO_x)_{Gaussian} = \frac{\int_{\bar{\varphi}-2s}^{\bar{\varphi}+2s} NO_x(\varphi_l)\, f(\varphi_l)\, d\varphi_l}{\int_{\bar{\varphi}-2s}^{\bar{\varphi}+2s} f(\varphi_l)\, d\varphi_l} \tag{4}$$

where $\int_{\bar{\varphi}-2s}^{\bar{\varphi}+2s} f(\varphi_l)\, d\varphi_l$ is approximately unity.

The integrations used 24 values of φ_l equally spaced between $\bar{\varphi}-2s$ and $\bar{\varphi}+2s$. The well-stirred-reactor program predicted corresponding NO_x values for each of these 24 equivalence ratios. All integrals were performed numerically by using either Simpson's rule, Newton's 3/8 rule, or a combination of these two rules (ref. 15). These theoretical NO_x values were then converted from parts per million by volume to emission indices, by the expressions discussed in reference 16, for comparison with the experimental data. In this conversion $\bar{\varphi}$ was used as the equivalence ratio needed for the calculations.

Experimental Calculations

The experimental data were obtained in a flametube rig by sampling the exhaust emissions 18 centimeters downstream from the flameholder, at the radial locations shown in figure 1. The local

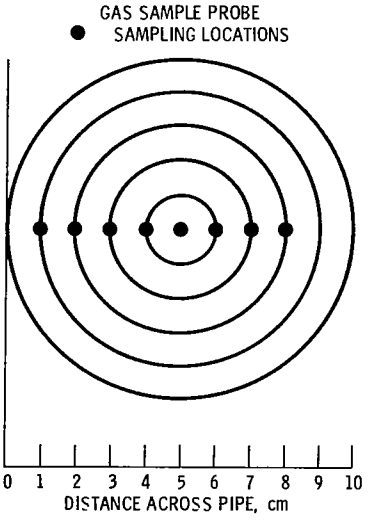

Figure 1. - Radial locations of data sampling points at a cross section of flametube rig combustion test section, 18 cm downstream of flameholder.

equivalence ratios were determined from a carbon balance of the sample exhaust species (ref. 16). How the average values of equivalence ratio and experimental NO_x level were determined is shown in figure 2. The quantity to be averaged Q is plotted as a function of pipe radius. A curve fit of the five data points from the pipe centerline to the pipe wall was used to determine 24 values of Q at equally spaced intermediate values of r (also shown in fig. 2). The curve-fit routine used a double three-point Lagrangian interpolation technique developed by Theodore Fessler of the NASA Lewis Research Center. This technique provides smooth curve fits by fitting two parabolas to the given data: one to the three points centered above the argument value, and one to the three points centered below it. A weighted average of these two values is the resulting interpolation. The Q values were mass weighted, and the average Q was found from

$$\overline{Q} = \frac{\int_0^{r_{max}} Qr\,dr}{\int_0^{r_{max}} r\,dr} \tag{5}$$

The experimental value of NO_x for a given fuel-air-ratio profile was found from

$$\overline{(NO_x)}_{exp} = \frac{\int_0^{r_{max}} (NO_x)_l r\,dr}{\int_0^{r_{max}} r\,dr} \tag{6}$$

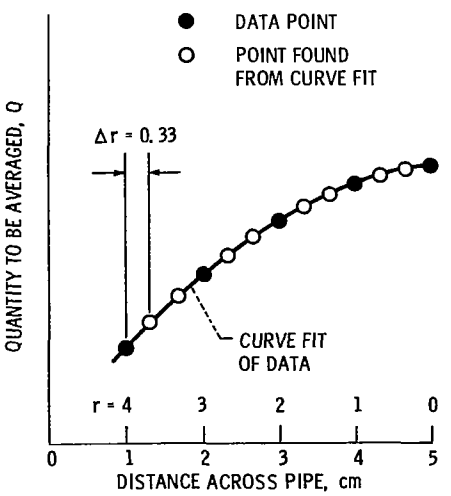

Figure 2. - Method of data averaging.

$\bar{Q} = \int_0^{r_{max}} Qr\,dr \Big/ \int_0^{r_{max}} r\,dr.$

where $(NO_x)_l$ is the locally measured NO_x value. The $(NO_x)_l$ values were in parts per million, and after the integration $\overline{(NO_x)}_{exp}$ was converted from parts per million to an emission index by using $\overline{\varphi}$ and the expressions of reference 16.

Apparatus and Procedure

The facility used for this set of experiments consisted of the closed-duct system shown in figure 3. The incoming air was heated to the three given inlet temperatures of 600, 700, and 800 K by a nonvitiating preheater. Reference velocity was determined from the total airflow rate, the inlet total temperature and pressure, and the combustor's cross-sectional flow area. The Jet A fuel was injected through the fuel injector mounted 26 centimeters upstream of the water-cooled, perforated-plate flameholder. Combustion occurred downstream of the flameholder in a water-cooled section that was instrumented to sample the combustion products in order to determine gaseous emissions.

Fuel Injector

The fuel injector that is shown in figure 4 consisted of 17 conical tubes, each with an upstream diameter of 1.3 centimeters and a half-angle of 7°. The tubes were 10.2 centimeters long. Fuel was injected at the air inlet end of each tube through a 0.5 millimeter-inside-diameter open-ended tube. Each fuel tube was 25.4 centimeters long. The five central fuel tubes were supplied through one control valve, and the outside ring of 12 tubes was supplied from a second control valve. A uniform fuel-air-ratio profile was produced by opening both valves fully. Various nonuniform profiles were produced by varying the amount of fuel flow to the two regions of the fuel injector by using these two valves. The overall equivalence ratio was determined from the fuel turbine flowmeter reading and the airflow rate as determined by a differential pressure measurement across a calibrated orifice. The overall equivalence ratio was maintained while the fuel-air-ratio profiles were changed. This fuel injector was the same fuel injector used in reference 17. In that study, it was shown that complete vaporization of the fuel was achieved at the conditions used here.

Flameholder

The water-cooled flameholder shown in figure 5 was made by welding sixty-one 0.6-centimeter-inside-diameter tubes between two 0.6-centimeter-thick stainless-steel plates. This flameholder produced a 75

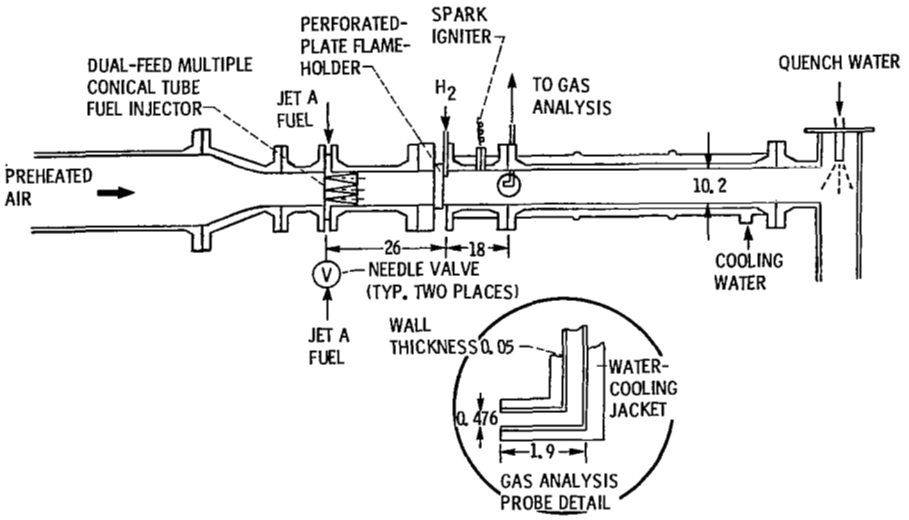

Figure 3. - Rig schematic. (All dimensions are in centimeters.)

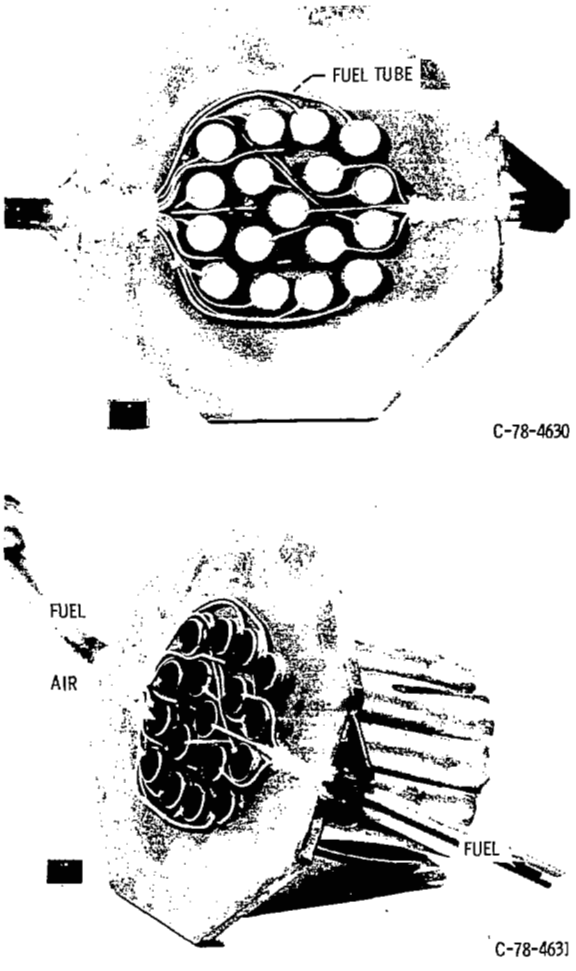

Figure 4. - Multiple conical tube injector.

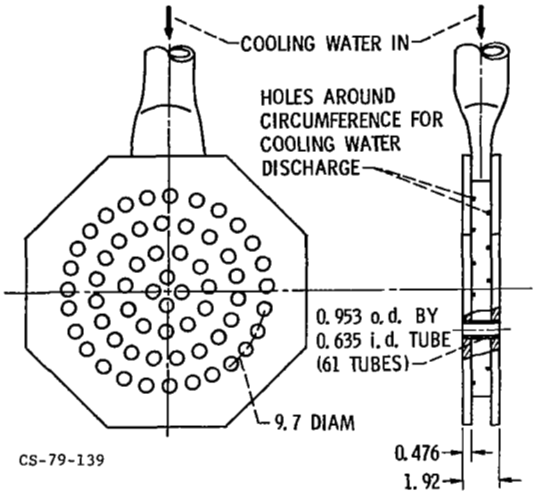

Figure 5. - Perforated-plate flameholder with 75 percent blockage. (All dimensions are in centimeters.)

percent blockage of the pipe cross-sectional area. Several Chromel-Alumel thermocouples were mounted on the upstream surface of the flameholder to detect any burning in the event of flashback or autoignition.

Combustor

The water-cooled combustor, shown in figure 3, (as well as the inlet duct) was 10.2 centimeters in diameter and 80 centimeters long. Quench water was injected downstream to cool the exhaust gases to about 370 K. The cooled exhaust then passed through

a remotely operated backpressure valve that controlled the rig pressure.

Gas Sampling

The combustion gases were sampled 18 centimeters downstream of the flameholder. The gas sample probe was made of 0.476-centimeter-diameter tubing surrounded by a water-cooling jacket, as shown in the insert of figure 3. The probe was traversed from the wall of the combustor section to the center, with gas samples being taken at 1-centimeter increments (fig. 1). Several readings were taken past the center in order to verify profile symmetry.

Stainless-steel tubing (0.95 cm diam) connected the gas sample probe to the gas analysis instrumentation. This 18-meter-long sample line was steam heated to maintain the sample gas temperature between 410 and 450 K. This prevented condensation of unburned hydrocarbons.

A flame ionization detector was used to measure the unburned hydrocarbons. Nondispersive infrared analyzers measured carbon monoxide and carbon dioxide concentrations. A chemiluminescence instrument measured the total NO_x concentrations. Instrument calibration was performed with standard calibration gases at the beginning of each day and also whenever a range change was made in a particular instrument.

Emissions measurements were converted from parts per million by volume to emission indices by the expressions discussed in reference 16.

Results and Discussion

Effect of Equivalence Ratio

Production of nitrogen oxides (NO_x) is a strong function of flame temperature (ref. 18), which varies with the fuel-air ratio, or equivalence ratio. The theoretical predictions of the average NO_x levels for uniform fuel-air-ratio profiles ($s=0$) and for progressively more nonuniform fuel-air-ratio profiles (increasing s) are shown in figure 6. The local NO_x values increased nearly exponentially with increasing φ_l for low values of φ_l. The NO_x level continued to increase until φ_l approached and exceeded stoichiometric (1.0), at which point the NO_x level decreased with further increase in φ_l. Consider now the effect of nonuniformity. For a given average equivalence ratio, say 0.6, a uniform profile ($s=0$) will have a φ_l of 0.6 everywhere in the duct. Thus the local NO_x level will everywhere correspond with that produced at a φ_l of 0.6. As nonuniformity is introduced (s increased), regions with φ_l greater than 0.6 and with φ_l less than 0.6 will appear.

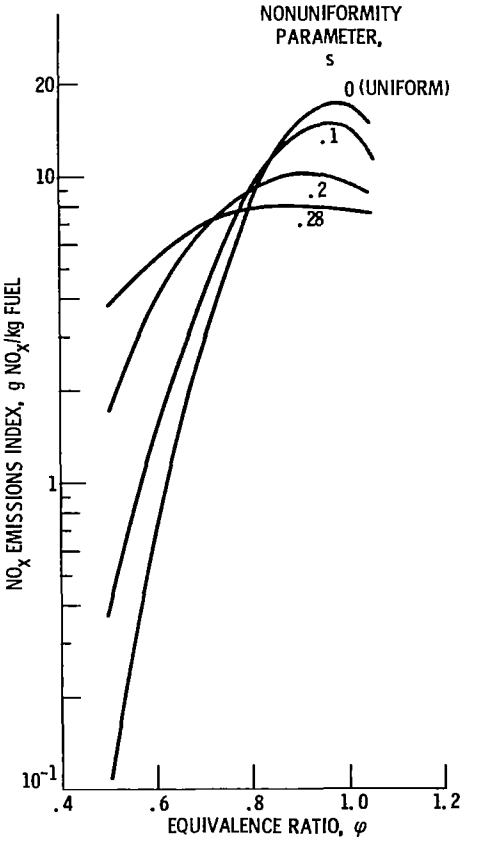

Figure 6. - Theoretical predictions of effect of equivalence ratio and fuel-air-ratio nonuniformity on NO_x emissions. Inlet air temperature, 600 K; rig pressure, 0.3 MPa; residence time, 0.002 sec.

From figure 6 a uniform profile having a $\overline{\varphi}$ of 0.6 would be expected to produce 0.75 gram of NO_x per kilogram of fuel (g NO_x/kg fuel). A nonuniform profile (e.g., $s=0.1$) would produce 1.45 g NO_x/kg fuel. Thus increasing s results in increasing average NO_x for this equivalence ratio.

For average equivalence ratios near stoichiometric, increased nonuniformity allows contributions from φ_l greater than 1.0 and from φ_l less than 1.0, which will tend to produce less NO_x than the uniform, stoichiometric profile (fig. 6). This figure shows that for average equivalence ratios less than 0.7 the trend is for increased NO_x levels with increased fuel-air-ratio nonuniformity. For average equivalence ratios near stoichiometric the trend shows decreasing NO_x with increasing nonuniformity. From this figure it is evident that the NO_x levels vary differently with s at each equivalence ratio.

Experimental Results

The six different fuel-air-ratio profiles studied at an inlet air temperature of 600 K are shown in figure 7. The average φ of 0.65 used in this experimental study is representative of the $\overline{\varphi}$ expected in a lean, premixed, prevaporized combustor. A combustor operating at a lower $\overline{\varphi}$ is less stable, but a higher $\overline{\varphi}$ will result in higher NO_x emissions. The corresponding NO_x and CO profiles that were measured are given in figures 8 and 9, respectively. Data were also taken at inlet air temperatures of 700 and 800 K and the results were similar. The degree of nonuniformity s of each fuel-air-ratio profile is given in each figure.

In figure 8, note that at an s of 0.024 (most uniform profile studied) the experimental NO_x value corresponded closely with the 1.5 g NO_x/kg fuel predicted in figure 6 at a φ of 0.65. The NO_x level varied little across the duct. The profile with an s of 0.090 approached stoichiometric at the 5-centimeter position (fig. 7); as expected, local NO_x was highest at 5 centimeters and the value of 12 g NO_x/kg fuel measured approached the predicted value of 17. Profiles in which φ_l was greater than 1.0 near the center of the duct resulted in lower-than-stoichiometric NO_x values in this region. Again, this trend can be seen to be consistent with the predicted effects of equivalence ratio on NO_x, as shown in figure 6.

The actual NO_x data may have differed from the predicted values as a result of the effects of diffusional mixing on the φ_l profiles. The NO_x values measured for a given φ_l profile may reflect the burning of a more sharply peaked φ_l distribution farther upstream. Another factor affecting NO_x peaks is the radiant heat losses from the high-temperature regions (near $\varphi_l = 1.0$), which cause lower local temperatures than expected and thus slightly lower NO_x levels.

The carbon monoxide data presented in figure 9 show that at 2 centimeters from the walls the CO levels reached a relative minimum for each profile. This position corresponds to the intersection of the φ_l curves (near $\varphi_l = 0.65$) shown in figure 7. Any deviation from this optimum φ produces more CO.

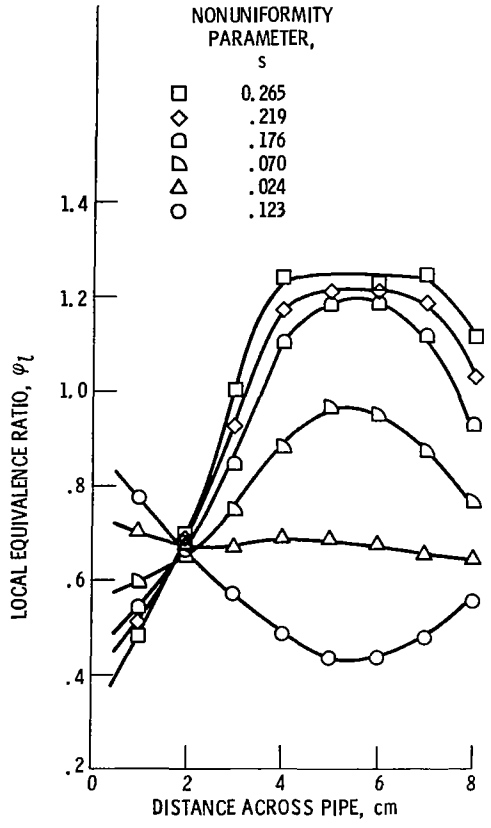

Figure 7. - Local equivalence ratio profiles. Inlet air temperature, 600 K; rig pressure, 0.3 MPa; average equivalence ratio, $\overline{\varphi}$, 0.65.

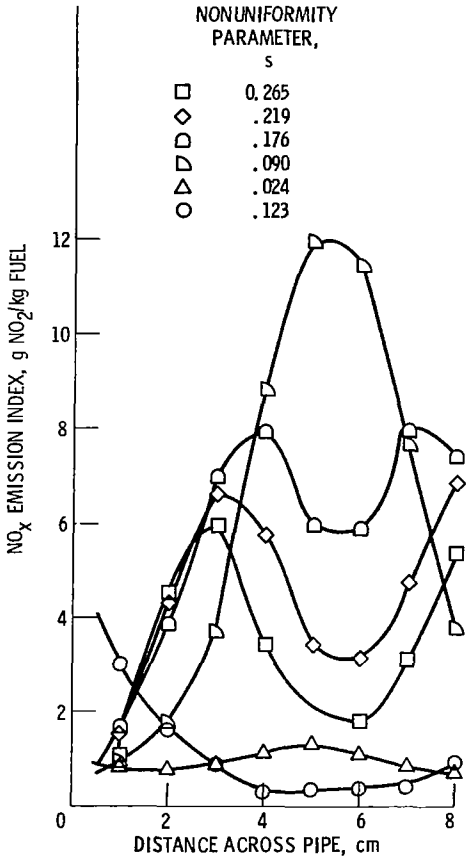

Figure 8. - Local NO_x emission index profiles. Inlet air temperature, 600 K; rig pressure, 0.3 MPa; average equivalence ratio, $\overline{\varphi}$, 0.65.

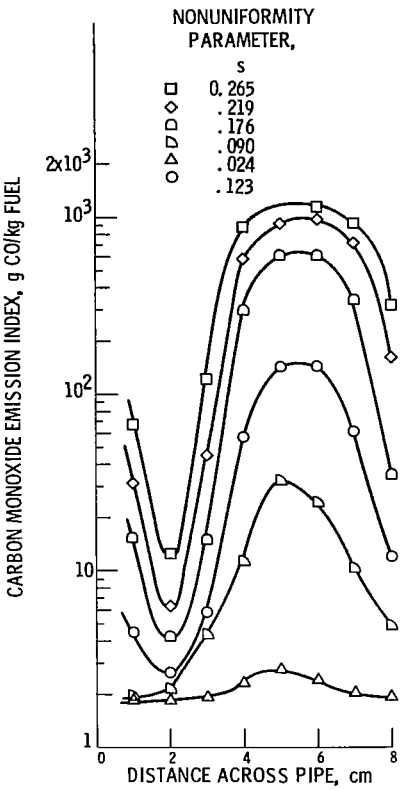

Figure 9. - Local carbon monoxide emission index profiles. Inlet air temperature, 600 K; rig pressure, 0.3 MPa; average equivalence ratio, $\bar{\varphi}$, 0.65.

This same equivalence ratio was seen to produce minimum CO in the experimental results of references 9 and 19, which used the same inlet conditions. For equivalence ratios less than 0.65 the low combustion efficiency produces more CO. For equivalence ratios greater than 0.65 greater amounts of equilibrium CO are produced. Although some CO values shown in figure 9 are somewhat below equilibrium (showing incomplete quenching in the probe), the relative values are still valid. Figure 9 also shows that the lowest CO level was produced for the most uniform profile. From this it is obvious that there is another benefit of attaining uniform fuel-air-ratio profiles: lower overall CO emissions.

Theoretical Results

The next six figures present the theoretical predictions of NO_x levels along with the experimental results. Figures 10 to 12 present sample NO_x profiles, and figures 13 to 15 present overall average NO_x values for each profile as a function of the nonuniformity parameter s for each profile.

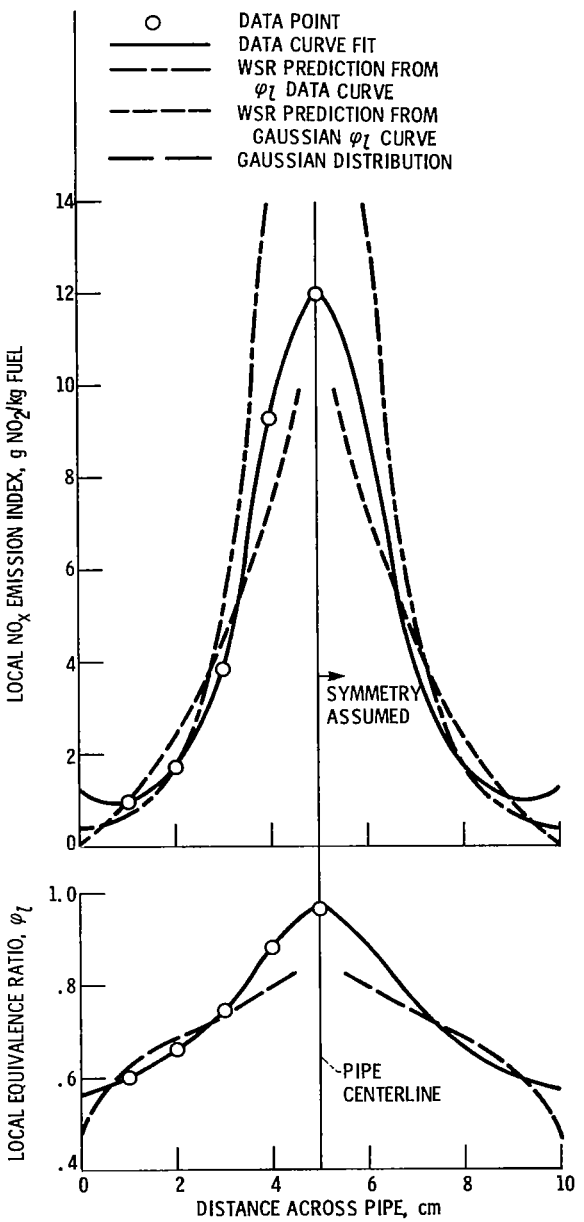

Figure 10. - Comparison of local experimental values with theoretical (well-stirred-reactor (WSR) program) predictions of equivalence ratio and NO_x emission index with 600 K and 0.3 MPa inlet air conditions - center-peaked fuel distribution. Average equivalence ratio, $\bar{\varphi}$, 0.650; nonuniformity parameter, s, 0.90.

Comparisons of the local experimental data points and the corresponding theoretical predictions are shown in figures 10 to 12 for an inlet air temperature of 600 K. Figure 10 shows a typical center-peaked fuel-air-ratio profile with a maximum φ_l less than stoichiometric (1.0). Figure 11 shows a circum-

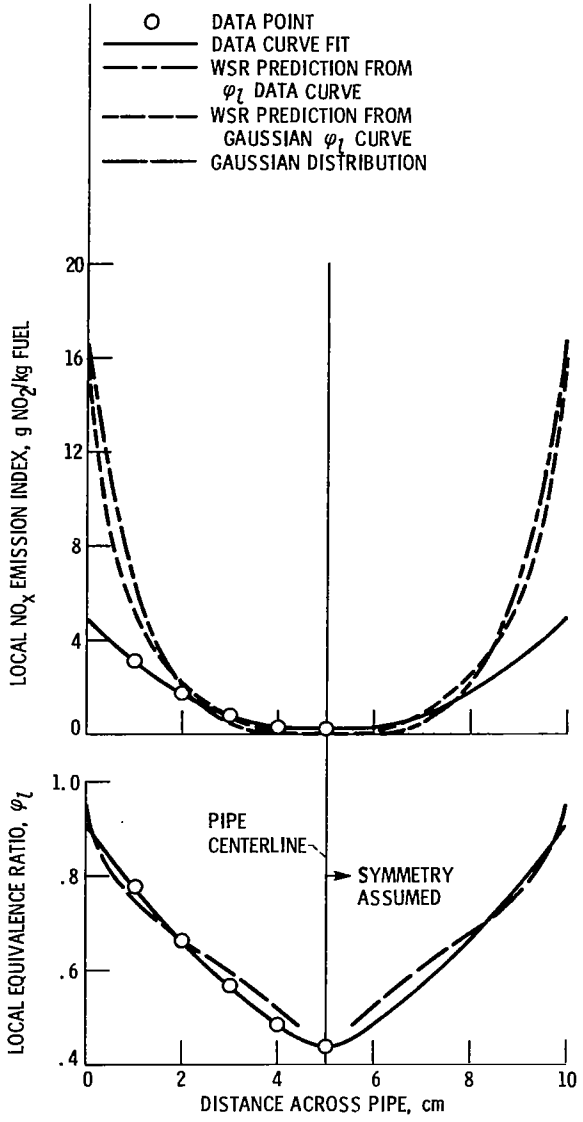

Figure 11. - Comparison of local experimental values with theoretical (well-stirred-reactor (WSR) program) equivalence ratio and NO_x emission index with 600 K and 0.3 MPa inlet air conditions - circumferentially peaked fuel distribution. Average equivalence ratio, $\bar{\varphi}$, 0.711; nonuniformity parameter, s, 0.123.

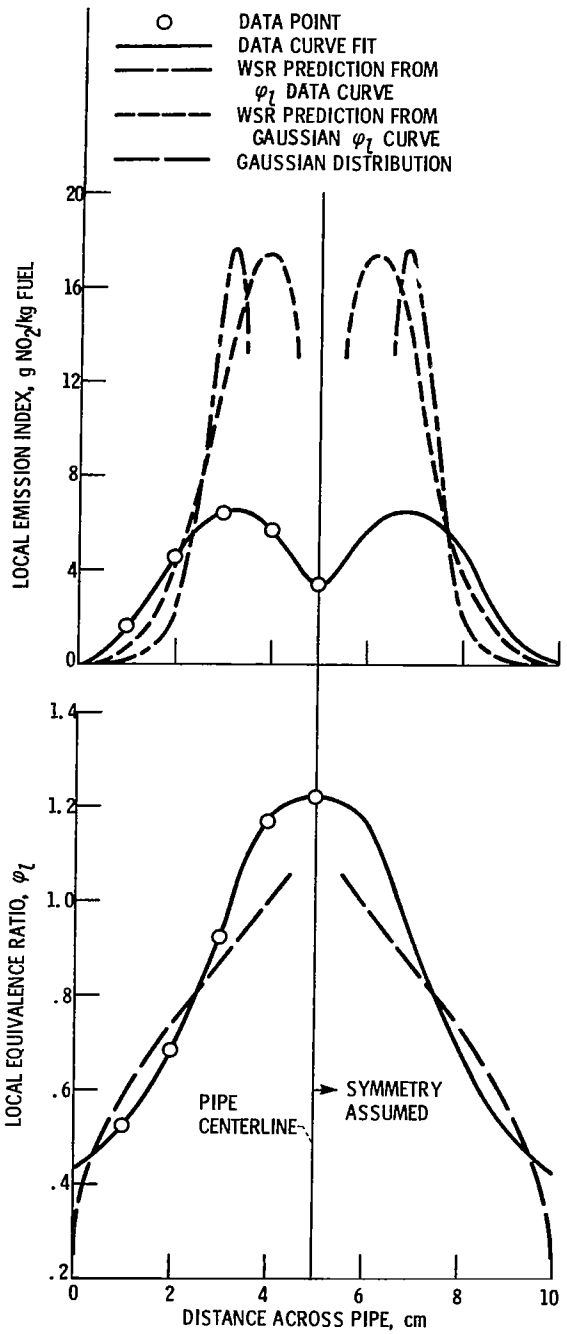

Figure 12. - Comparison of local experimental values with theoretical (well-stirred-reactor (WSR) program) predictions of equivalence ratio and NO_x emission index with 600 K and 0.3 MPa inlet air conditions - center-peaked fuel distribution. Average equivalence ratio, $\bar{\varphi}$, 0.657; nonuniformity parameter, s, 0.219.

ferentially peaked profile. Figure 12 again shows a center-peaked profile; however, it represents a case where the peak values are greater than stoichiometric.

A center-peaked fuel-air-ratio profile with its Gaussian approximation is shown in the lower portion of figure 10. The upper curves in the figure are the corresponding local NO_x values. The NO_x data, with the curve fit, are shown. The well-stirred-reactor program (ref. 14) predicted NO_x values from the φ_l data curve and from the φ_l Gaussian curve as shown. For all these curves symmetry was assumed about the pipe centerline, as shown in the figure.

The same format is presented in figure 11, where a circumferentially peaked fuel-air-ratio profile is

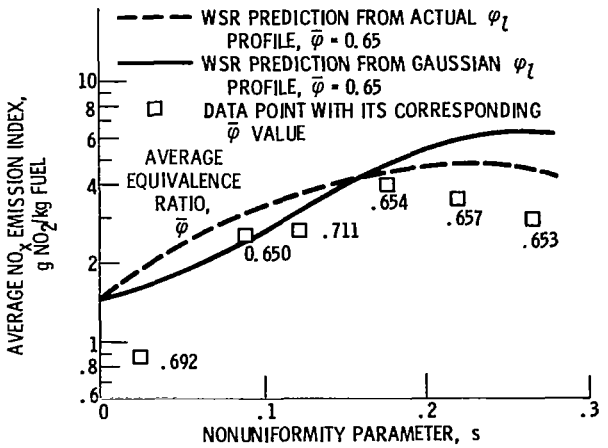

Figure 13. - Comparison of average NO_x values, experimentally determined, with theoretical (well-stirred-reactor (WSR) program) predictions at 600 K and 0.3 MPa inlet air conditions.

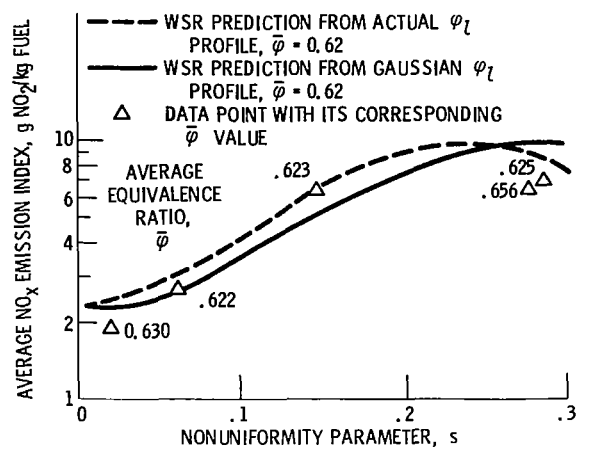

Figure 14. - Comparison of average NO_x values, experimentally determined, with theoretical (well-stirred-reactor (WSR) program) predictions at 700 K and 0.3 MPa inlet air conditions.

shown. The theoretical predictions agree quite well for this case. It can be seen that, as expected, the low φ_l values produce relatively low NO_x values.

In figure 12 a center-peaked profile is again shown. However, this figure shows a highly nonuniform (s=0.219) fuel-air-ratio profile so that the local equivalence ratio exceeds 1.0 (stoichiometric). The resulting NO_x profile shows two peaks near a φ_l of 1.0. Unlike figures 10 and 11, where the theory corresponds fairly well with the data, figure 12 shows some discrepancy near the two NO_x peaks. As discussed previously in regard to figure 8, peaks may be flattened in experimental situations as a result of cooling and diffusion effects that are not considered in the theoretical analysis. Since these peaks occur

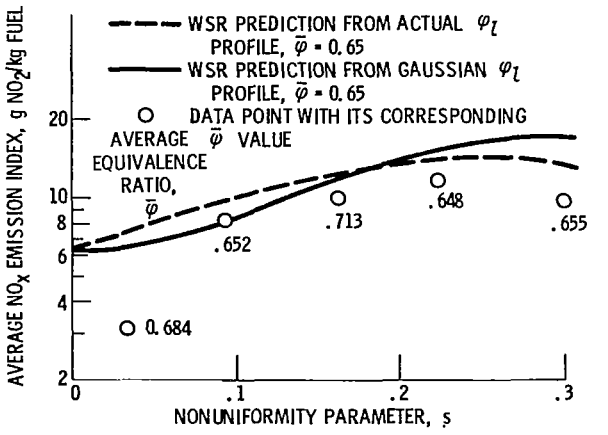

Figure 15. - Comparison of average NO_x values, experimentally determined, with theoretical (well-stirred-reactor (WSR) program) predictions at 800 K and 0.3 MPa inlet air conditions.

near the pipe centerline, these values are weighted less than the more accurately predicted areas nearer the walls, so the average NO_x values are still reasonably well approximated by the theory. Comparisons were also made at inlet air temperatures of 700 and 800 K, with similar results.

The Gaussian fuel-air-ratio profile assumption appears to be a good approximation of the local experimental data. In figures 13 to 15 average NO_x values are shown as a function of s for the well-stirred-reactor prediction from the measured φ_l profile and the Gaussian φ_l profile along with the experimentally determined NO_x values for the three inlet air temperatures 600, 700, and 800 K. The average experimental NO_x values are shown as data points in these figures along with their corresponding average equivalence ratios. Some of these average equivalence ratios are somewhat different from the others. One possible reason for this is that although the metered fuel flow rate remained the same, the assumption of fuel-air-ratio profile symmetry may not be as accurate for some profiles as for others. Also, the measurements near the wall were weighted more highly than those in the center. Finer measurements taken near the wall may have produced more accurate values for $\overline{\varphi}$. In drawing the curves for the theoretical predictions, average equivalence ratios near the majority of the experimental values were used, and these average equivalence ratios are indicated in the figures.

The two theoretical NO_x curves shown in figures 13 to 15 are the average NO_x values predicted by the well-stirred-reactor program from the Gaussian φ_l profile and from the actual φ_l data profile. The data points shown are the average experimental NO_x values. Both curves approximate the data fairly well

and thus justify the use of the Gaussian φ_l profile assumption. For the 600 K case presented in figure 13 discrepancies between theory and the experimental results are consistent with the results in figures 10 to 12. Figure 10, which illustrates a case in which s is 0.09, shows the NO_x data falling generally between the two theoretical curves. The overall NO_x value calculated for the $\bar{\varphi}=0.65$ and $s=0.090$ case shown in figure 13 also falls between the two theoretical curves. Because of the flattening of NO_x peaks in the experimental results the maximum measured NO_x values are lower than the theoretical predictions in figures 11 and 12. The average experimental NO_x values corresponding to these curves ($s=0.123$ and $s=0.219$) are lower than predicted in figure 13 also.

The Gaussian theoretical predictions for NO_x emissions at inlet air temperatures of 600, 700, and 800 K are shown in figure 16 for an average equivalence ratio of 0.65. The same trend of producing increased NO_x with increasing nonuniformity is found at all three inlet air temperatures. This trend continues until an s value of approximately 0.2 is reached; at which point a larger amount of overstoichiometric burning occurs and less NO_x is produced.

The results of this report can be used to estimate the degree of fuel-air-ratio nonuniformity required in the fuel preparation section of actual engines in order to meet NO_x standards. For example, if it were desirable to meet a NO_x goal of 3 g NO_x/kg fuel, figure 16 can be used to determine the degree of nonuniformity permitted for a primary-zone equivalence ratio of 0.65. For inlet conditions of 600 K and 0.3 MPa, a value of s less than 0.08 would be needed to achieve this goal. At 700 K and 0.3 MPa, an s less than 0.05 would be required. At 800 K and 0.3 MPa this goal cannot be achieved with a primary-zone equivalence ratio of 0.65.

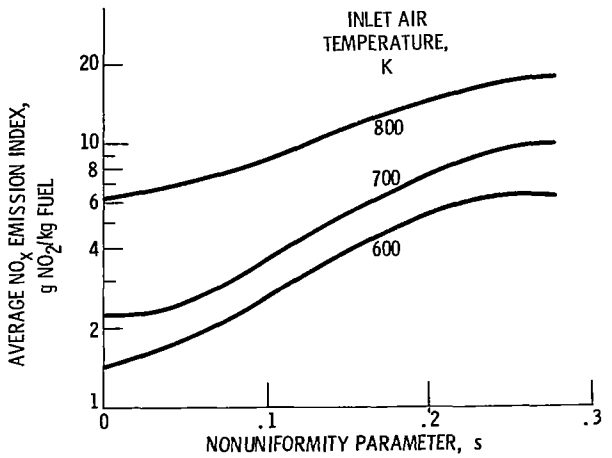

Figure 16. - Well-stirred-reactor program prediction of average NO_x values from Gaussian equivalence ratio profiles at 600, 700, and 800 K, 0.3 MPa inlet air conditions. Average equivalence ratio, $\bar{\varphi}$, 0.65.

Concluding Remarks

The NO_x levels for nonuniform fuel-air-ratio profiles were successfully predicted by an analytical method and verified by experimental data. From the results of this study greater understanding of lean, premixed, prevaporized combustion has been achieved. The results show that lean, premixed, prevaporized combustors may need very uniform fuel-air distributions to achieve low NO_x emissions.

Summary of Results

The effect of fuel-air-ratio nonuniformity on NO_x emissions was analytically and experimentally investigated, with particular interest for lean, premixed, prevaporized combustion. The conditions studied were inlet air temperatures of 600, 700, and 800 K, a rig pressure of 0.3 MPa, and an inlet air velocity of 25 meters per second. Jet A fuel was injected through a dual-zoned fuel injector and premixed with air so that six profiles of fuel-air mixtures were produced at each inlet air temperature. Gas sample measurements were taken downstream of a perforated-plate flameholder.

From this study the following results are summarized:

1. For average equivalence ratios less than 0.7, average NO_x emissions increased with increasing fuel-air-ratio profile nonuniformity.
2. For average equivalence ratios near stoichiometric, average NO_x emissions decreased with increasing fuel-air-ratio profile nonuniformity.
3. For any value of the nonuniformity parameter, NO_x emissions decreased with decreasing average equivalence ratio for average equivalence ratios less than 0.7.
4. Inlet air temperatures between 600 and 800 K had no effect on the trends of the effect of nonuniformity on NO_x emissions.
5. Both the magnitude and trends of the experimental data agree with the analytical predictions of the average NO_x emissions for various degrees of nonuniformity, inlet air temperatures, and average equivalence ratios.

Lewis Research Center
National Aeronautics and Space Administration
Cleveland, Ohio, January 23, 1981

References

1. Grobecker, A. J.; Coronite, S. C.; and Cannon, R. H., Jr.: Report of Findings: The Effect of Stratospheric Pollution by Aircraft. DOT-TST-75-50, Department of Transportation, 1974.
2. Roberts, P. B.; White, D. J.; and Shekleton, J. R.: Advanced Low NO_x Combustors for Supersonic High-Altitude Aircraft Gas Turbines. (RDR-1814, Solar Division of International Harvester; NASA Contract NAS3-18028.) NASA CR-134889, 1975.
3. Gleason, C. C.; Rogers, D. W.; and Bahr, D. W.: The Experimental Clean Combustor Program – Phase II. (R76AEG422, General Electric Co.; NASA Contract NAS3-18551.) NASA CR-134971, 1976.
4. Roberts, R.; Peduzzi, A.; and Vitti, G. E.: The Experimental Clean Combustor Program – Phase II. (PWA-5418, Pratt & Whitney Aircraft; NASA Contract NAS3-18544.) NASA CR-134969, 1976.
5. Dodds, W. J.; Gleason, C. C.; and Bahr, D. W.: Aircraft Gas Turbine Low-Power Emissions Reduction Program. (R78AEG408, General Electric Co.; NASA Contract NAS3-20580.) NASA CR-135434, 1978.
6. Anderson, D. N.: Effect of Premixing on Nitric Oxide Formation. NASA TM X-68220, 1973.
7. Marek, C. J.; and Papathakos, L. C.: Exhaust Emissions from a Premixing, Prevaporizing Flame Tube Using Jet A Fuel. NASA TM X-3383, 1976.
8. Anderson, D. N.: Effects of Equivalence Ratio and Dwell Time on Exhaust Emissions from an Experimental Premixing, Prevaporizing Burner. NASA TM X-71592. 1974.
9. Roffe, G.: and Venkataramani, K. S.: Emission Measurements for a Lean Premixed Propane/Air System at Pressures up to 30 Atmospheres. (GASL-TR-250, General Applied Science Labs., Inc.; NASA Contract NAS3-20603.) NASA CR-159421, 1978.
10. Roffe, G.; and Venkataramani, K. S.: Experimental Study of the Effects of Flameholder Geometry on Emissions and Performance of Lean Premixed Combustors. (GASL-TR-249, General Applied Science Labs., Inc.; NASA Contract NAS3-20603.) NASA CR-135424, 1978.
11. Semerjian, H. G.: and Ball, I. C.: Potential Reduction in NO_x Emissions with Premixed Combustors. Presented at the Combustion Institute, Central States Section, Spring Technical Meeting, Cleveland, Ohio, March 28-30, 1977.
12. Mularz, E. J.: Lean, Premixed, Prevaporized Combustion for Aircraft Gas Turbine Engines. NASA TM-79148, 1979.
13. Mikus, T., Heywood, J. B.; and Hicks, R. E.: Nitric Oxide Formation in Gas Turbine Engines: A Theoretical and Experimental Study. NASA CR-2977, 1978.
14. Boccio, J. L.; Weilerstein, G.; and Edelman, R. B.: A Mathematical Model for Jet Engine Combustor Pollutant Emissions. (GASL-TR-781, General Applied Science Labs., Inc.; NASA Contract NASW-2235.) NASA CR-121208, 1973.
15. TSS Programmers Manual, Volume II. NASA Lewis Research Center, 1972.
16. Procedure for the Continuous Sampling and Measurement of Gaseous Emissions from Aircraft Turbine Engines. SAE Aerospace Recommended Practice 1256, Oct. 1971.
17. Cooper, L. P.: Effect of Degree of Fuel Vaporization upon Emissions for a Premixed Partially Vaporized Combustion System. NASA TP-1582, 1980.
18. Touchton, D. L.; and Dibelius, N. R.: A Correlation of Nitrogen Oxides Emissions with Gas Turbine Operating Parameters. ASME Paper 76-GT-14, Mar. 1976.
19. Roffe, G.; and Venkataramani, K. S.: Experimental Study of the Effect of Cycle Pressure on Lean Combustion Emissions. NASA CR-3032, 1978.

Bibliography

Control on Air Pollution From Aircraft and Aircraft Engines. Federal Register, Vol. 43, No. 58, Pt, III. Fri., Mar. 24, 1978, pp. 12613-12634.

Jones, R. E.; et al.: Results and Status of the NASA Aircraft Engine Emission Reduction Technology Programs. NASA TM-79009, 1978.

1. Report No.	2. Government Accession No.	3. Recipient's Catalog No.
NASA TP-1798		

4. Title and Subtitle	5. Report Date
EFFECT OF FUEL-AIR-RATIO NONUNIFORMITY ON EMISSIONS OF NITROGEN OXIDES	November 1981
	6. Performing Organization Code 505-32-32
7. Author(s) Valerie J. Lyons	8. Performing Organization Report No. E-648
	10. Work Unit No.
9. Performing Organization Name and Address National Aeronautics and Space Administration Lewis Research Center Cleveland, Ohio 44135	11. Contract or Grant No.
	13. Type of Report and Period Covered Technical Paper
12. Sponsoring Agency Name and Address National Aeronautics and Space Administration Washington, D.C. 20546	14. Sponsoring Agency Code

15. Supplementary Notes

16. Abstract

An analytical and experimental study was performed to determine how inlet fuel-air-ratio profile nonuniformity affects NO_x emissions. The theoretical NO_x levels were verified in a flametube rig at inlet air temperatures of 600, 700, and 800 K, a rig pressure of 0.3 MPa, a reference velocity of 25 m/sec, an overall equivalence ratio of 0.6, and a residence time near 0.002 sec. The theory predicts an increase in NO_x emissions with increased fuel-air-ratio profile nonuniformity for average equivalence ratios less than 0.7 and a decrease in NO_x emissions for average equivalence ratios near stoichiometric. The results of this report can be used to predict the degree of uniformity of fuel-air-ratio profiles that is necessary to achieve NO_x emissions goals for actual engines that use lean, premixed, prevaporized combustion systems.

17. Key Words (Suggested by Author(s))	18. Distribution Statement
Fuel-air ratios; Fuel combustion; Combustion products; Combustion physics; Air pollution; Nitric oxide; Nonuniformity; Oxides of nitrogen	Unclassified - unlimited STAR Category 07

19. Security Classif. (of this report)	20. Security Classif. (of this page)	21. No. of Pages	22. Price*
Unclassified	Unclassified	13	A02

* For sale by the National Technical Information Service, Springfield, Virginia 22161

NASA-Langley, 1981

National Aeronautics and Space Administration

Washington, D.C.
20546

Official Business
Penalty for Private Use, $300

SPECIAL FOURTH CLASS MAIL
BOOK

Postage and Fees Paid
National Aeronautics and
Space Administration
NASA-451

5 1 1U,A, 102981 S00903DS
DEPT OF THE AIR FORCE
AF WEAPONS LABORATORY
ATTN: TECHNICAL LIBRARY (SUL)
KIRTLAND AFB NM 87117

NASA

POSTMASTER: If Undeliverable (Section 158 Postal Manual) Do Not Return